t-$\bar{t}$ PRODUCTION NEAR THRESHOLD

WITH pNRQCD

ANTONIO PINEDA

(IFAE, U. Autònoma Barcelona)

Motivation

Motivation

t–$\bar{t}$ near threshold production region: $E_{cm} \simeq 340 - 360$ GeV. Nonrelativistic system

$$v_{top} = \sqrt{1 - \frac{4m_t^2}{s}} \ll 1$$

$$m_t \gg m_t v_{top} \gg m_t v_{top}^2$$

$$\frac{\alpha_s}{v_{top}} \sim 1 \rightarrow \text{Coulomb resummation} \rightarrow \text{Schroedinger equation}$$

$$\text{LO} \sim \sum_{n=0}^{\infty} c_n \frac{\alpha_s^n}{v_{top}^n}$$

$$\text{NLO} \sim \sum_{n=0}^{\infty} c_n \frac{\alpha_s^n}{v_{top}^n} \times (\alpha_s, v_{top})$$

$$\ldots\ldots$$

Motivation

t–$\bar{t}$ near threshold production region: $E_{cm} \simeq 340 - 360$ GeV. Nonrelativistic system

$$v_{top} = \sqrt{1 - \frac{4m_t^2}{s}} \ll 1$$

$$m_t \gg m_t v_{top} \gg m_t v_{top}^2$$

$$\frac{\alpha_s}{v_{top}} \sim 1 \rightarrow \text{Coulomb resummation} \rightarrow \text{Schroedinger equation}$$

$$\text{LL} \sim \sum_{n=0}^{\infty} c_n \frac{\alpha_s^n}{v_{top}^n} \sum_{m=0}^{\infty} d_m \alpha_s^m \ln^m v$$

$$\text{NLL} \sim \sum_{n=0}^{\infty} c_n \frac{\alpha_s^n}{v_{top}^n} \sum_{m=0}^{\infty} d_m \alpha_s^m \ln^m v \times (\alpha_s, v_{top})$$

$$\ldots\ldots$$

Motivation

t–$\bar{t}$ near threshold production region: $E_{cm} \simeq 340 - 360$ GeV. Nonrelativistic system

$$v_{top} = \sqrt{1 - \frac{4m_t^2}{s}} \ll 1$$

$$m_t \gg m_t v_{top} \gg m_t v_{top}^2$$

$$\frac{\alpha_s}{v_{top}} \sim 1 \rightarrow \text{Coulomb resummation} \rightarrow \text{Schroedinger equation}$$

$$\text{LL} \sim \sum_{n=0}^{\infty} c_n \frac{\alpha_s^n}{v_{top}^n} \sum_{m=0}^{\infty} d_m \alpha_s^m \ln^m v$$

$$\text{NLL} \sim \sum_{n=0}^{\infty} c_n \frac{\alpha_s^n}{v_{top}^n} \sum_{m=0}^{\infty} d_m \alpha_s^m \ln^m v \times (\alpha_s, v_{top})$$

$$\cdots\cdots$$

Summing logs in non-relativistic systems

Large logs understood as ratios of scales: $\ln(mv/m) \sim \ln \alpha_s$, $\ln(mv^2/(mv)) \sim \ln \alpha_s$.
Resummation of logs: $(\alpha_s \ln)^n$.

$$\begin{aligned}
\delta E &\sim m\alpha_s^4 + m\alpha_s^5 \ln \alpha_s + m\alpha_s^6 \ln^2 \alpha_s + \cdots \\
\Gamma(V_Q(nS) \rightarrow e^+e^-) &\sim m\alpha_s^3(1 + \alpha_s^2 \ln \alpha_s + \alpha_s^3 \ln^2 \alpha_s + \cdots) \\
\Gamma(P_Q(nS) \rightarrow \gamma\gamma) &\sim m\alpha_s^3(1 + \alpha_s^2 \ln \alpha_s + \alpha_s^3 \ln^2 \alpha_s + \cdots)
\end{aligned}$$

NR Effective Field Theories

Our aim is to provide a systematic method to deal with NR bound state systems. We will introduce a hierarchy of EFTs when sequentially integrating out each scale (only one scale in each step, strong simplification).

QCD

↓ Integrating out the hard scale (m)

NRQCD — Caswell, Lepage; Bodwin, Braaten, Lepage

↓ Integrating out the soft scale (mv)

pNRQCD — Soto, Pineda

$$\left(i\partial_0 - \frac{\mathbf{p}^2}{2m} - V_0(r)\right)\Phi(\mathbf{r}) = 0$$
+corrections to the potential
+interaction with other low energy degrees of freedom

} potential NRQCD $\quad \mathrm{E} \sim \mathrm{mv}^2$

In the perturbative case the starting point is $V_0 = -C_f\frac{\alpha}{r}$. pNRQCD has two ultraviolet cut-offs, ν_p and ν_{us}. ν_{us} fulfils the relation $\mathbf{p}^2/m \ll \nu_{us} \ll |\mathbf{p}|$ and is the cut-off of the energy of the quarks, and of the energy and the momentum of the gluons. ν_p fulfils $|\mathbf{p}| \ll \nu_p \ll m$ and is the cut-off of the relative momentum of the quark–antiquark system, $\mathbf{p}$.

Nonrelativistic Sum rules (b-$\bar{b}$, c-$\bar{c}$), t-$\bar{t}$ production near threshold

Determination of m_b, m_t, α_s, Higgs-top yukawa coupling, ...

$$J^\mu = \bar{Q}\gamma^\mu Q = B_1 \psi^\dagger \boldsymbol{\sigma} \chi + \cdots ,$$

$$B_1 = 1 + a_1 \alpha_s + a_2 \alpha_s^2 + \cdots$$

B_1 at NNLO: Hoang(QED); Beneke, Signer, Smirnov; Czarnecki, Melnikov
B_1, B_0 at NLL: Pineda; Hoang, Stewart
B_1/B_0 at NNLL: Penin, Pineda, Smirnov, Steinhauser
B_1, B_0 at NNLL (partial): Pineda, Signer

$$(q_\mu q_\nu - g_{\mu\nu})\Pi(q^2) = i \int d^4x e^{iqx} \langle \mathrm{vac}|J_\mu(x) J_\nu(0)|\mathrm{vac}\rangle$$

$$\Pi(q^2) \sim B_1^2 \langle \mathbf{r}=\mathbf{0}| \frac{1}{E-H} |\mathbf{r}=\mathbf{0}\rangle$$

$$G(0,0,E) = \sum_{m=0}^{\infty} \frac{|\phi_{0m}(0)|^2}{E_{0m} - E + i\epsilon - i\Gamma_t} + \frac{1}{\pi} \int_0^\infty dE' \frac{|\phi_{0E'}(0)|^2}{E_{0E'} - E + i\epsilon - i\Gamma_t}$$

A NNLL renormalization group improved expression of $M(V_Q(nS))$ is also needed in order to obtain expressions for the t-$\bar{t}$ production near threshold with NNLL accuracy:
$M(V_Q(nS))$ at NNLL: Pineda; Hoang, Stewart
$M(V_Q(nS)) - M(P_Q(nS))$ at NNNLL: Kniehl, Penin, Pineda, Smirnov, Steinhauser

Relation of the vacuum polarization with $\sigma_{t\bar{t}}$, non-relativistic sum rules and $\Gamma(V_Q(nS) \to e^+e^-)$

$$\Gamma(V \to e^+e^-) \sim \frac{1}{m^2} B_1^2 |\phi(\mathbf{0})|^2$$

$$\sigma_{t-\bar{t}} \sim B_1(\nu)^2 \mathrm{Im} G(0,0,\sqrt{s}) + \cdots$$

$$M_n \equiv \frac{12\pi^2 e_b^2}{n!} \left(\frac{d}{dq^2}\right)^n \Pi(q^2)|_{q^2=0} = \int_0^\infty \frac{ds}{s^{n+1}} R_{b\bar{b}}(s),$$

$$M_n = 48\pi e_b^2 N_c \int_{-\infty}^{\infty} \frac{dE}{(E+2m_b)^{2n+3}} \left(B_1^2 - B_1 d_1 \frac{E}{3m_b}\right) \mathrm{Im}\, G(0,0,E)$$

The top mass

Next Linear Collider. $\delta m_t(\text{exp.}) \lesssim 30$ MeV; decay width 2%: Martinez-Miquel

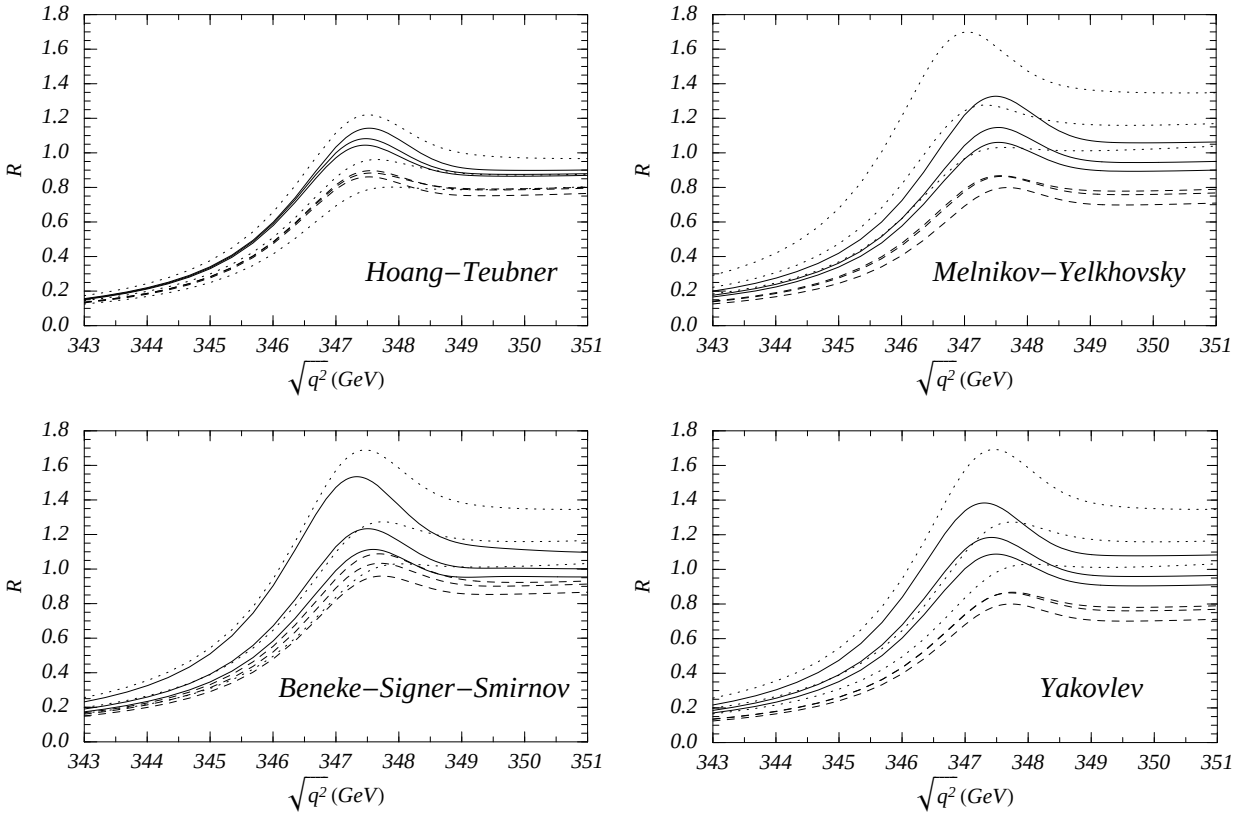

Figure 1:

Total normalized photon induced $t\bar{t}$ cross section at the Internation Linear Collider versus the center of mass energy at LO (dotted line), NLO (dashed line) and NNLO (solid line). Hoang-Teubner used the 1S scheme with $m_t^{1S} = 173.68$ GeV, Melnikov–Yelkhovsky the kinetic mass $m^{\text{kin}}_{t,15\,\text{GeV}} = 173.10$ GeV, and Beneke–Signer–Smirnov and Yakovlev the PS mass $m^{\text{PS}}_{t,20\,\text{GeV}} = 173.30$ GeV. Plot from hep-ph/0001286.

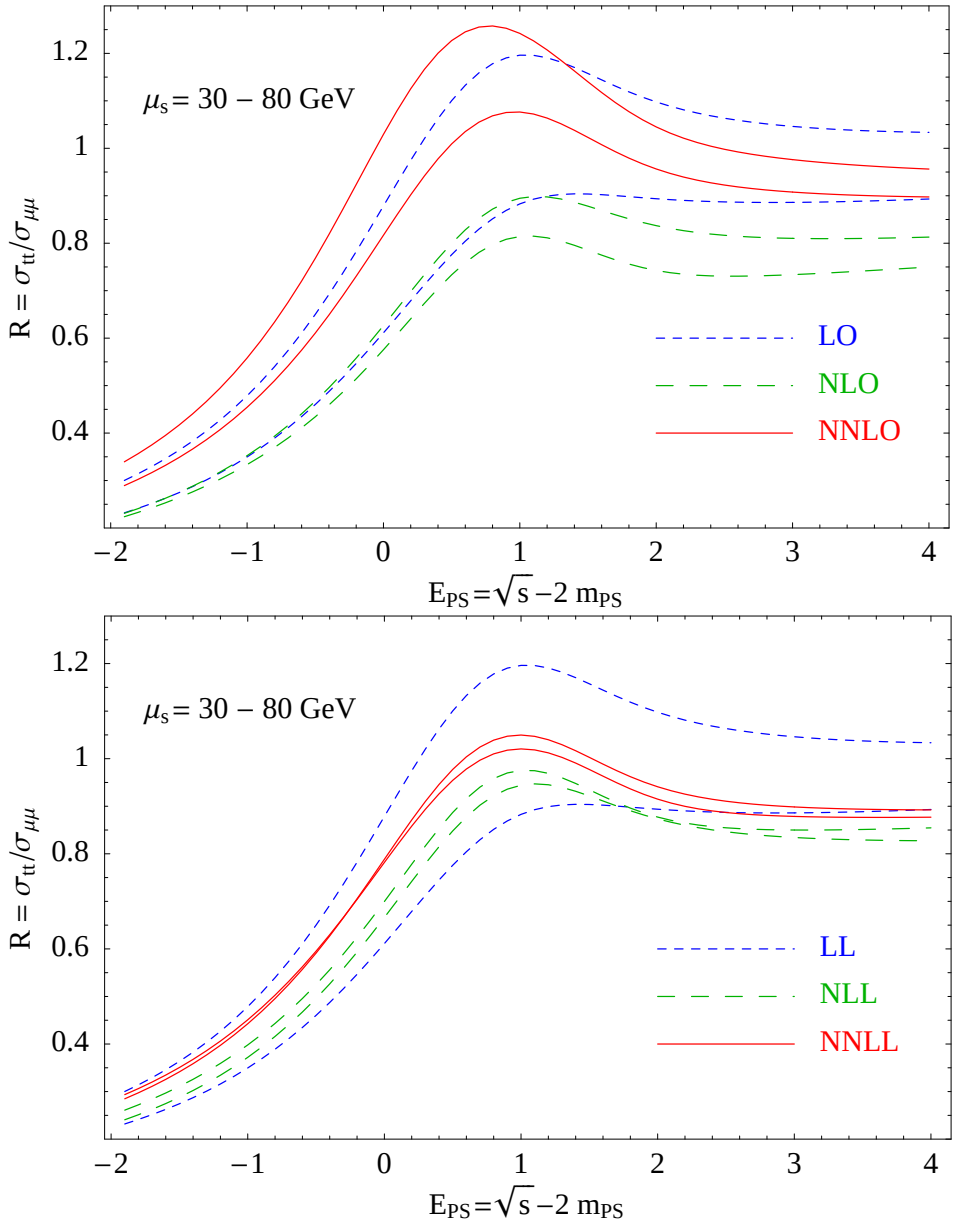

Figure 2: Threshold scan for $t\bar{t}$ using the PS mass, $m_{\rm PS}(20\,{\rm GeV}) = 175$ GeV. The upper panel shows the fixed order results, LO, NLO and NNLO, whereas in the lower panel the RGI results LL, NLL and NNLL are displayed. The soft scale is varied from μ_s=30 GeV to μ_s=80 GeV. Pineda-Signer

The RGI significantly reduces the scale dependence and improves the convergence.

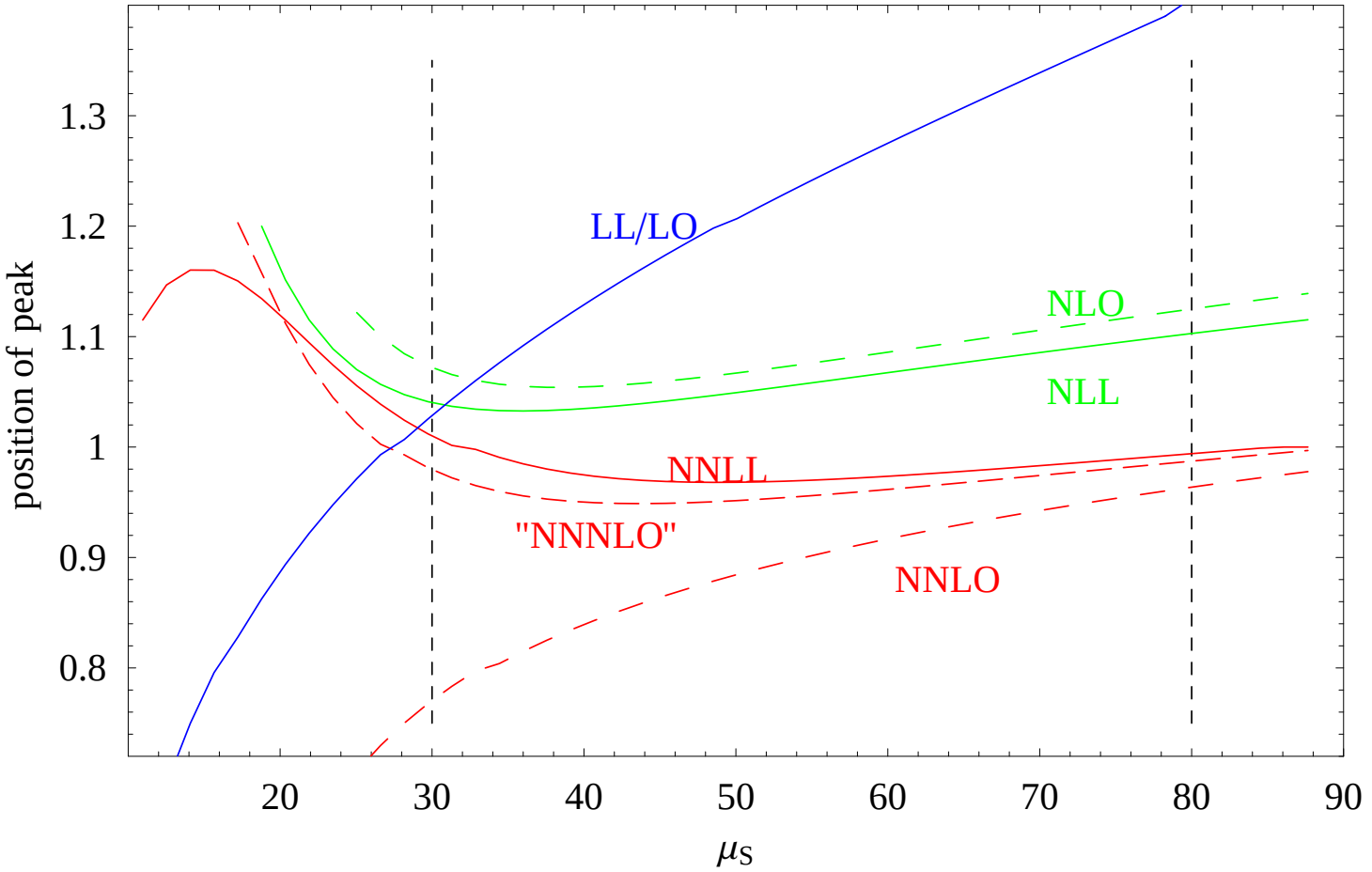

Figure 3: The position of the peak of the RGI threshold cross section as a function of the soft scale μ_s. The vertical dashed lines show the limits of variation used in Figure 2.

Contrary to previous claims, to get an improved determination of the top mass RGI has to be used (or "NNNLO").

Leading logs seem to give the dominant contribution

Strong scale dependence for scales below 30 GeV

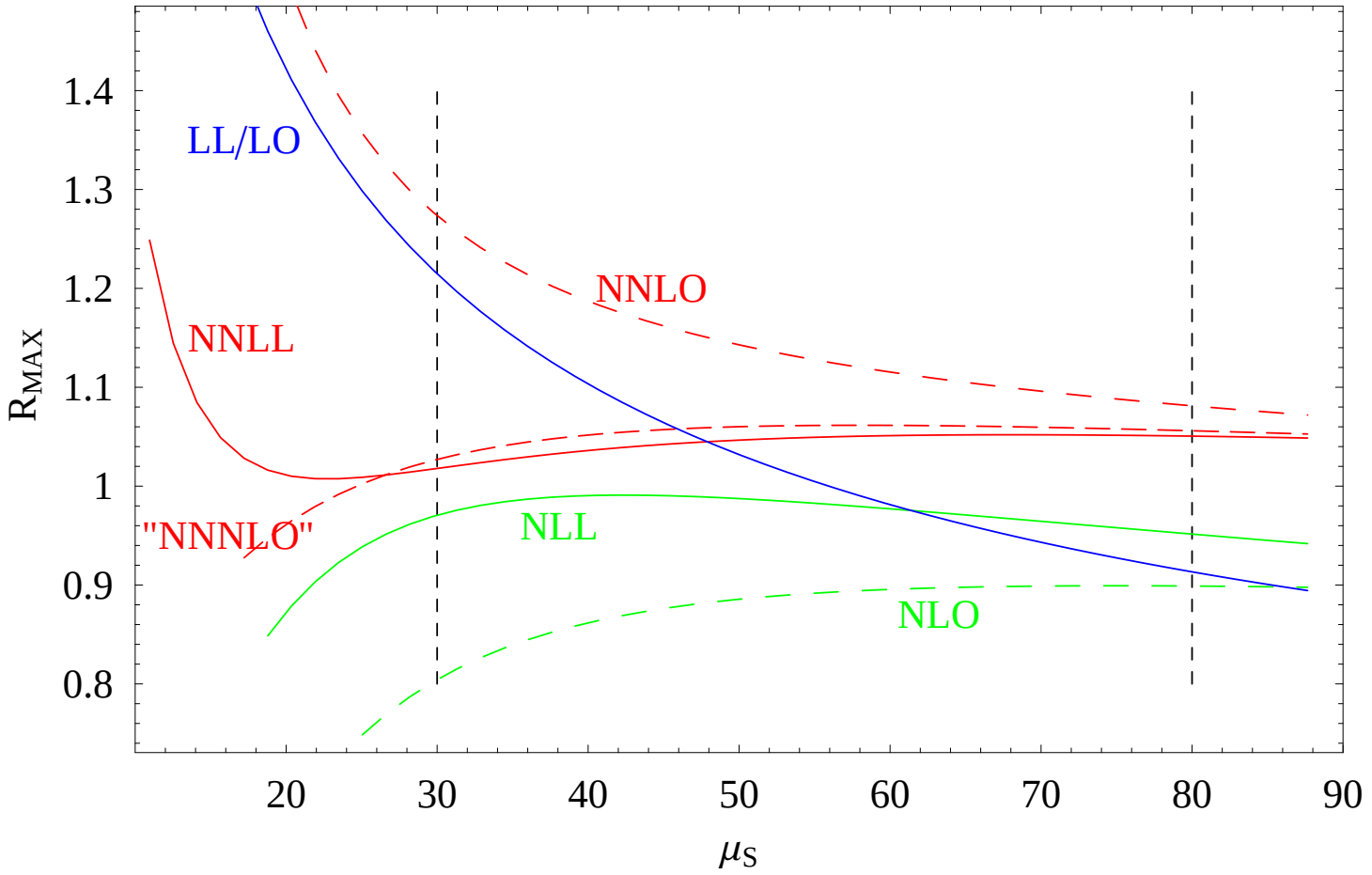

Figure 4: The normalization of the peak of the RGI threshold cross section as a function of the soft scale μ_s. The vertical dashed lines show the limits of variation used in Figure 2.

To get an improved determination of the normalization the RGI is compulsory (NLL and NNLL).

Leading logs seem to give the dominant contribution

Strong scale dependence for scales below 30 GeV

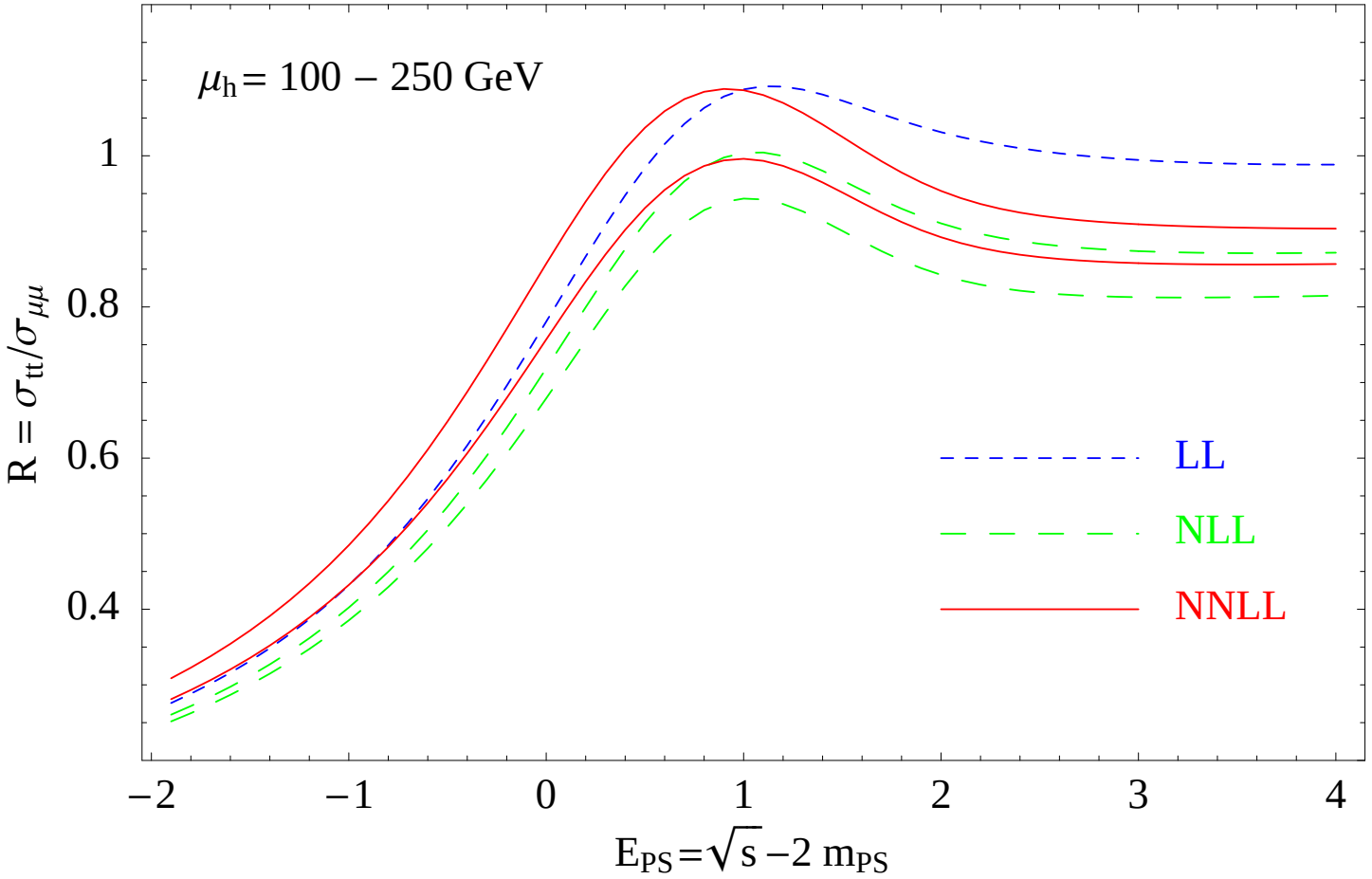

Figure 5: Dependence of the $t\bar{t}$ threshold scan on the hard scale μ_h, using the PS mass. At NNLL (NLL) the lower (upper) curve corresponds to $\mu_h = 250$ GeV, whereas the upper (lower) curve corresponds to $\mu_h = 100$ GeV. Pineda-Signer

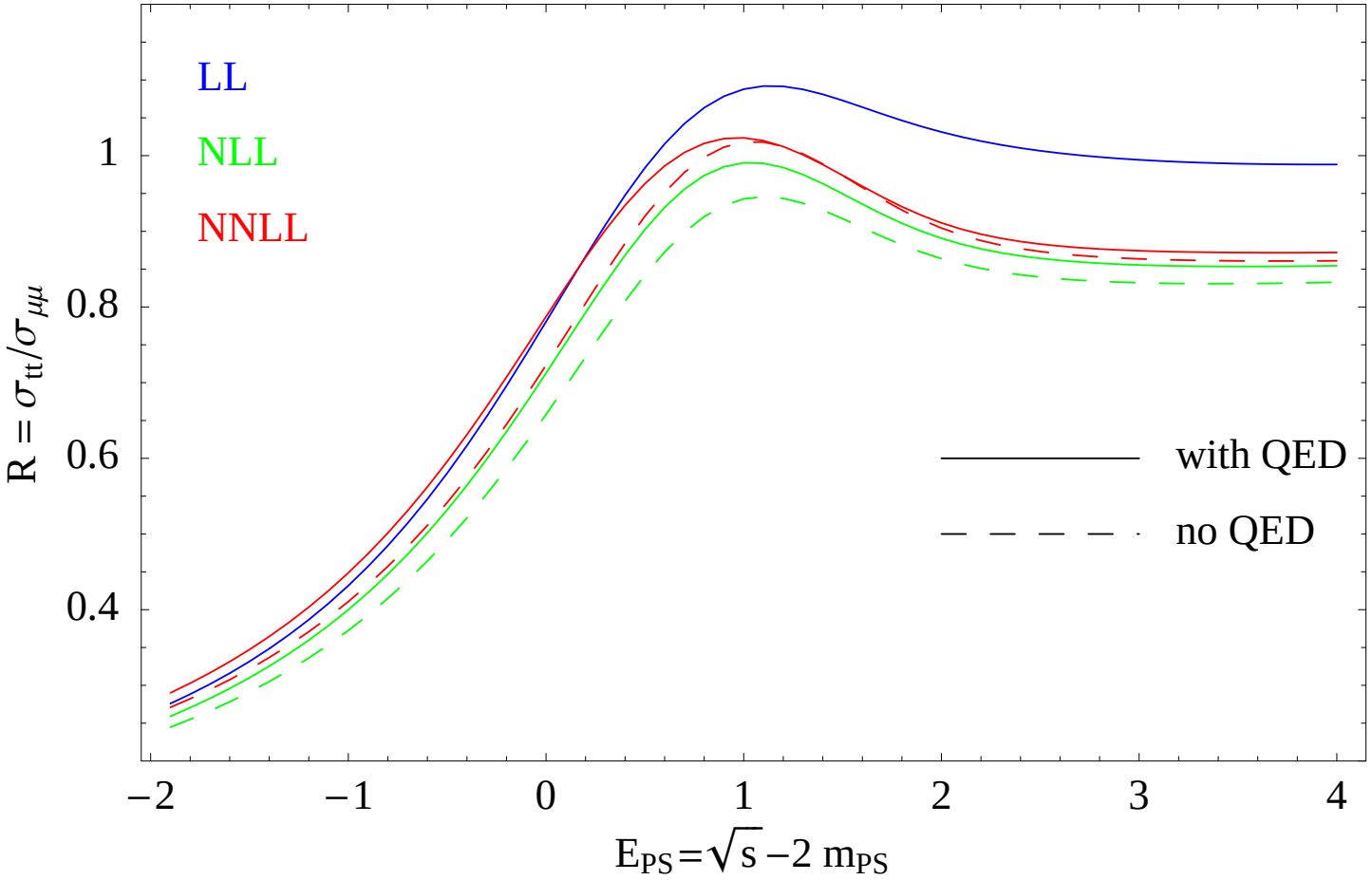

Figure 6: Effects of the QED corrections to the $t\bar{t}$ threshold scan. The hard ans soft sales are chosen as $\mu_h = m_{\rm PS} = 175$ GeV and $\mu_s = 40$ GeV. Pineda-Signer

Error on top mass (position of the peak): ~ 100 MeV

Error on the normalization of the total cross section: $\sim 10\%$

Decay Ratio at NNLL

Penin, Smirnov, Steinhauser, Pineda

$$\frac{\Gamma(V_Q(nS)\to e^+e^-)}{\Gamma(P_Q(nS)\to\gamma\gamma)} \sim 1+\alpha\ln\alpha+\alpha^2\ln^2\alpha+\cdots$$
$$+\alpha+\alpha^2\ln\alpha+\alpha^3\ln^2\alpha+\cdots$$
$$+\alpha^2+\alpha^3\ln\alpha+\alpha^4\ln^2\alpha+\cdots$$

$$\frac{\Gamma(T(1S)\to e^+e^-)}{\Gamma(\eta_t(1S)\to\gamma\gamma)} = \frac{1}{3Q_t^2}\left(1-0.13198-0.0179492\right) .$$

$$\frac{\Gamma(\Upsilon(1S)\to e^+e^-)}{\Gamma(\eta_b(1S)\to\gamma\gamma)} = \frac{1}{3Q_b^2}\left(1-0.302-0.111\right) .$$

$$\Gamma(\eta_b(1S)\to\gamma\gamma) = 0.659\pm 0.089(\text{th.})^{+0.019}_{-0.018}(\delta\alpha_s)\pm 0.015(\text{exp.})\ \text{KeV} ,$$

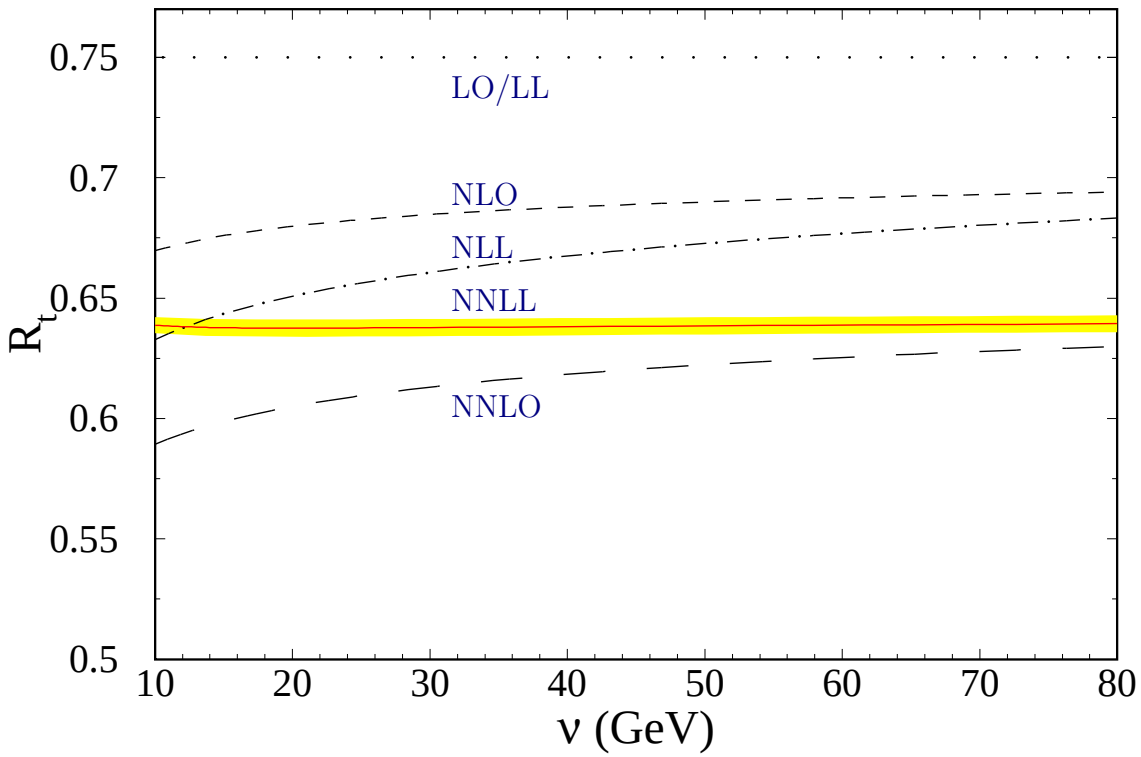

Figure 7: The spin ratio as the function of the renormalization scale ν in LO (dotted line), NLO (short-dashed line), NNLO (long-dashed line), LL (dotted line), NLL (dot-dashed line), and NNLL (bold solid line) approximation for the (would be) toponium ground state with $\nu_h = m_t$. For the NNLL result the band reflects the errors due to $\alpha_s(M_Z) = 0.118 \pm 0.003$

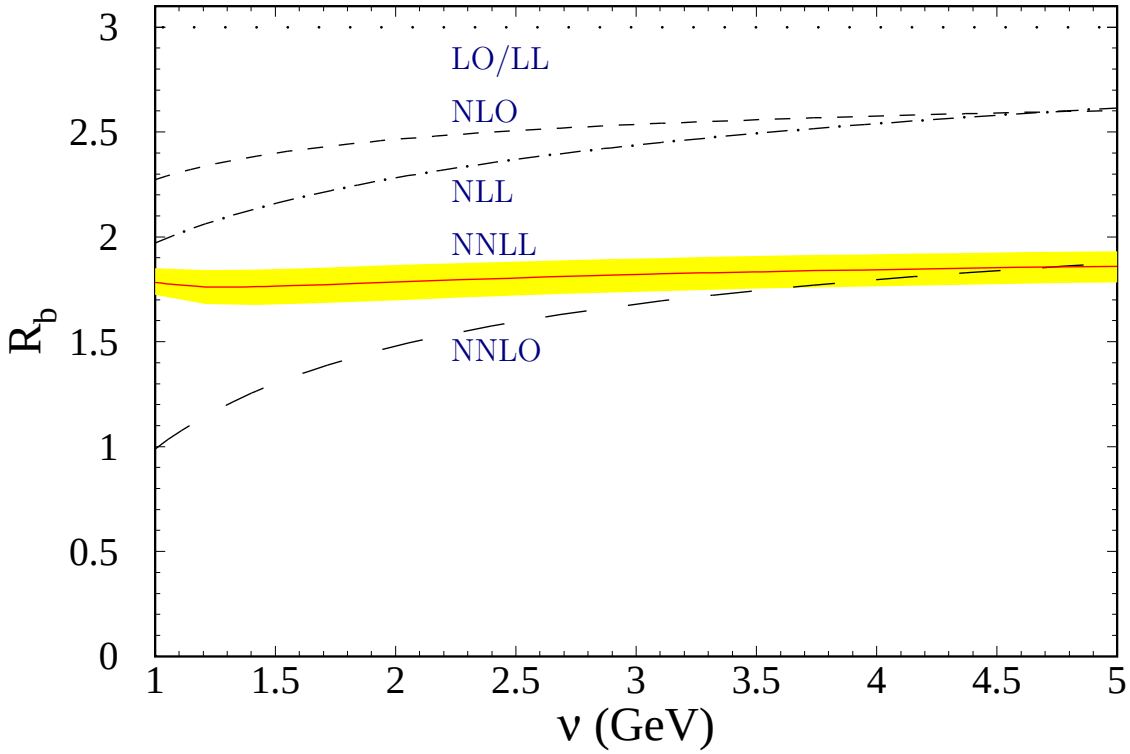

Figure 8: The spin ratio as the function of the renormalization scale ν in LO (dotted line), NLO (short-dashed line), NNLO (long-dashed line), LL (dotted line), NLL (dot-dashed line), and NNLL (bold solid line) approximation for the bottomonium ground state with $\nu_h = m_b$. For the NNLL result the band reflects the errors due to $\alpha_s(M_Z) = 0.118 \pm 0.003$

Inclusive electromagnetic decays: bottomonium

Pineda-Signer

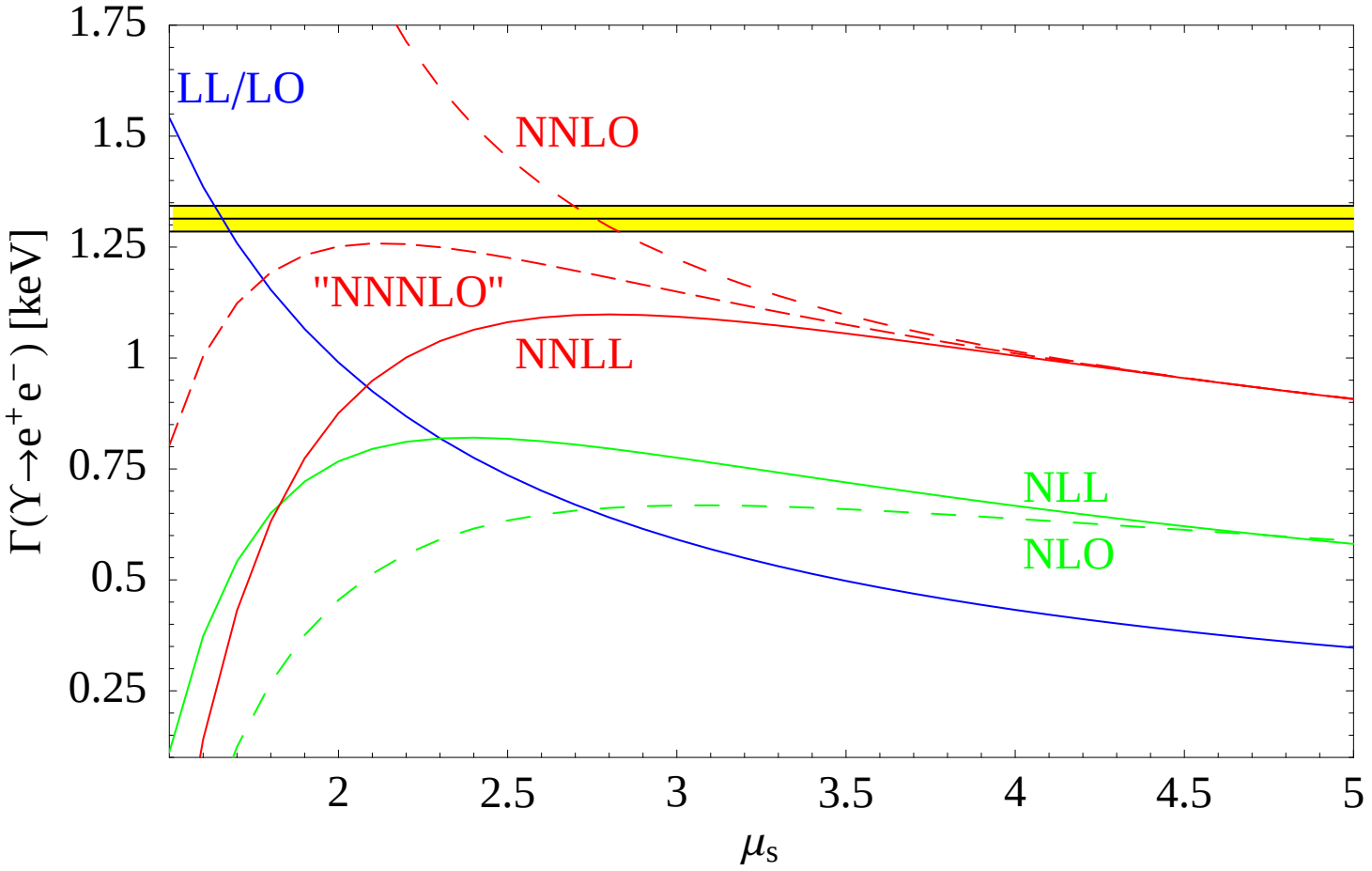

Figure 9: Prediction for the $\Upsilon(1S)$ decay rate to e^+e^-. We work in the RS' scheme.

The effect of the resummation of logarithms is important if compared with just keeping the single logarithm.

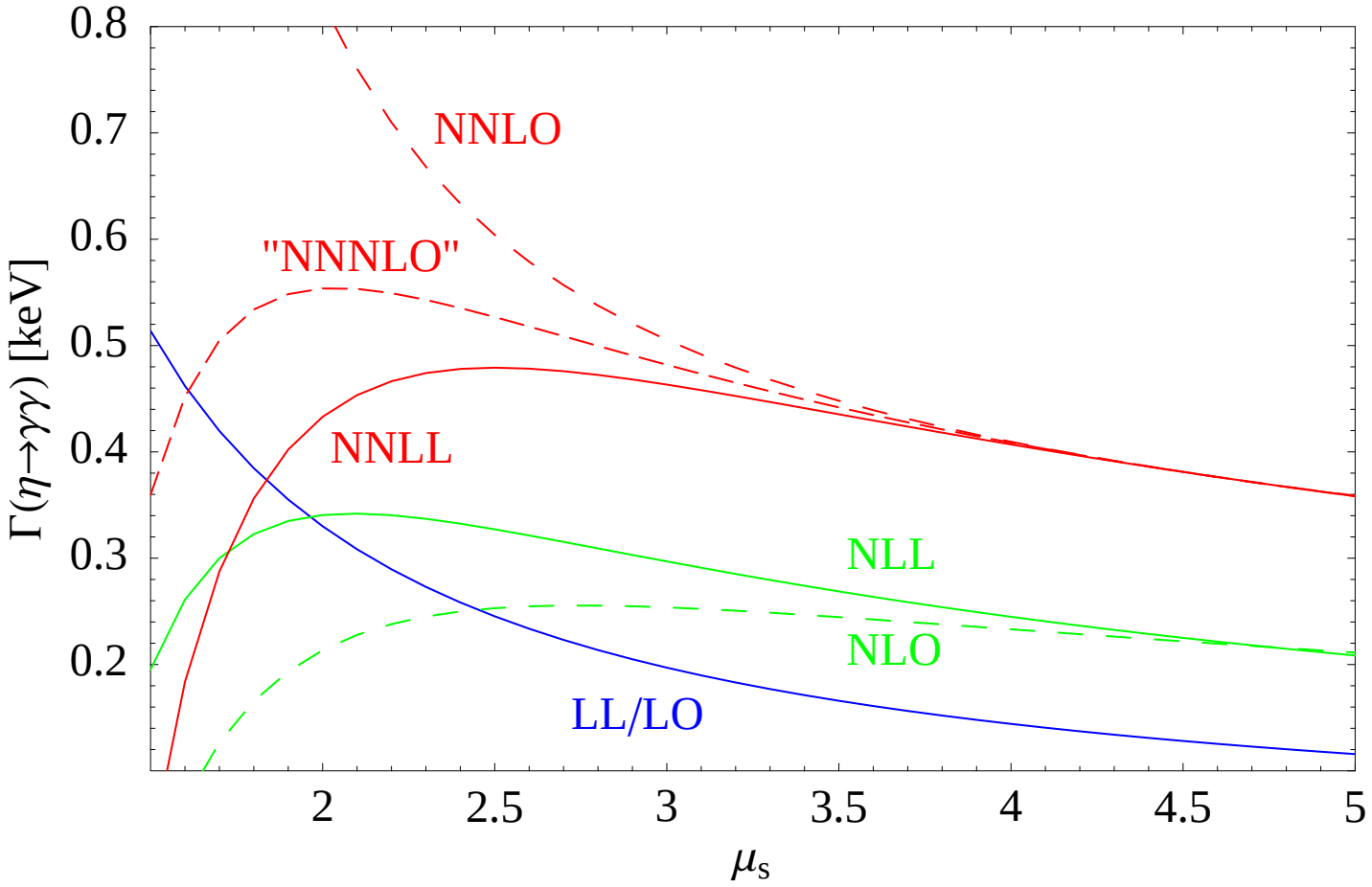

Figure 10: Prediction for the $\eta_b(1S)$ decay rate to two photons. We work in the RS' scheme.

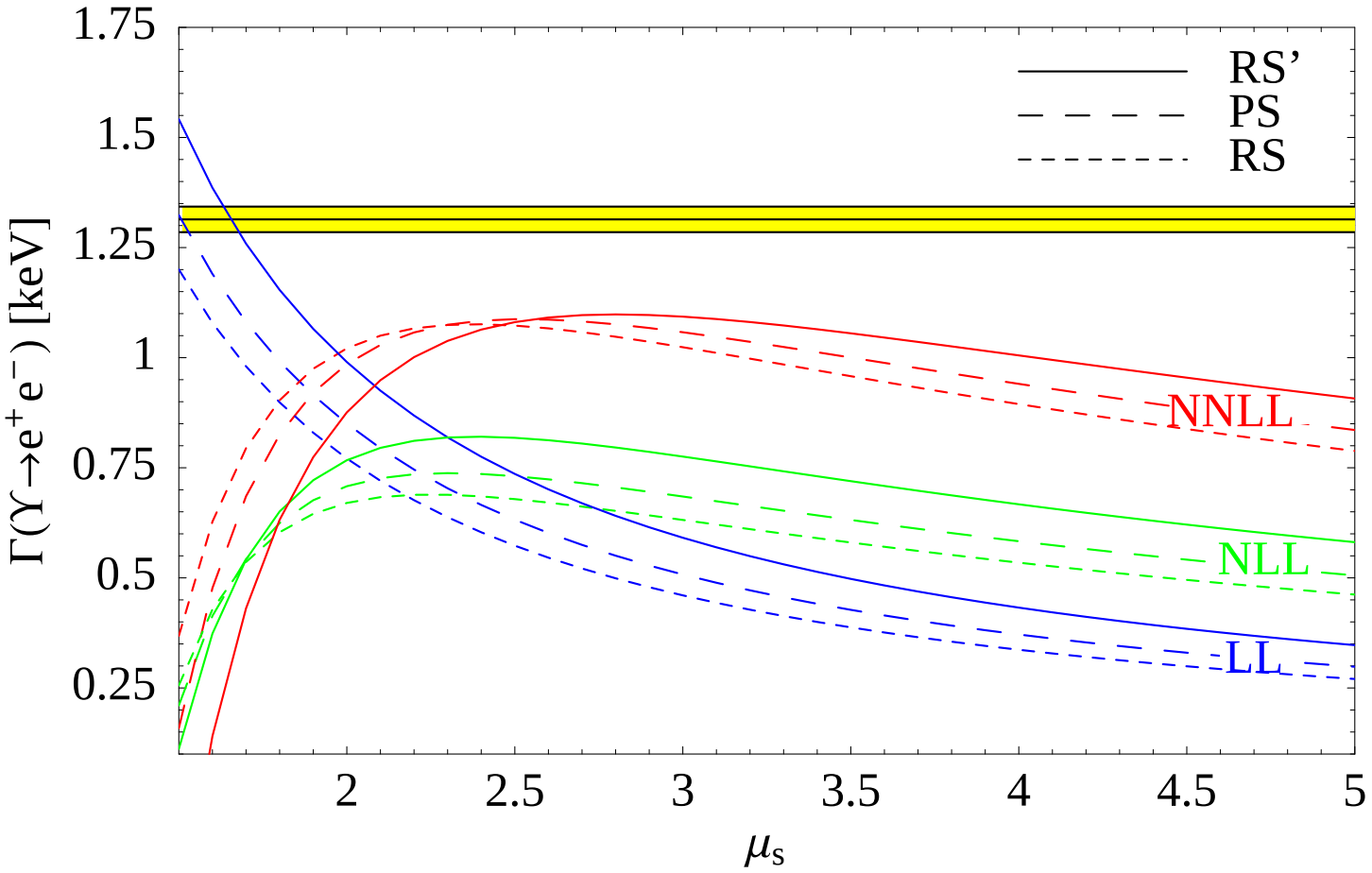

Figure 11: Prediction for the $\Upsilon(1S)$ decay rate to e^+e^- at LL, NLL and NNLL for the PS, RS and RS' mass.

The effects due to the change of scheme are small. Other sources of error are much larger.

Non-relativistic Sum rules: bottomonium

Pineda-Signer

$$M_n \equiv \frac{12\pi^2 e_b^2}{n!}\left(\frac{d}{dq^2}\right)^n \Pi(q^2)|_{q^2=0} = \int_0^\infty \frac{ds}{s^{n+1}} R_{b\bar{b}}(s),$$

$$M_n = 48\pi e_b^2 N_c \int_{-\infty}^{\infty} \frac{dE}{(E+2m_b)^{2n+3}}\left(B_1^2 - B_1 d_1 \frac{E}{3m_b}\right) \mathrm{Im}\, G(0,0,E)$$

n	$m_{b,\mathrm{PS}}(2\ \mathrm{GeV})$	Δ_{th}	Δ_{exp}	Δ_α	Δ_{tot}	$\overline{m}_b$
6	4460	40	50	35	70	4135 ± 65
8	4505	45	25	30	60	4170 ± 55
10	4515	45	15	25	55	4185 ± 50
12	4520	45	10	20	50	4185 ± 45
14	4520	40	10	15	45	4185 ± 40
n	$m_{b,\mathrm{RS}}(2\ \mathrm{GeV})$	Δ_{th}	Δ_{exp}	Δ_α	Δ_{tot}	$\overline{m}_b$
6	4315	55	50	25	80	4140 ± 70
8	4360	65	30	20	75	4180 ± 65
10	4370	65	20	10	70	4190 ± 60
12	4370	65	15	5	65	4190 ± 60
14	4370	65	10	5	65	4185 ± 55

Table 1: *Extraction of $m_{b,\mathrm{PS/RS}}(2\ GeV)$ with errors for various n. All values are given in MeV and rounded to 5 MeV. The total error has been obtained by adding the partial errors in quadrature. The corresponding value for the $\overline{\mathrm{MS}}$ mass with its error is given in the last column.*

small $n \longrightarrow$ larger experimental error (not to use theoretical ansatz above threshold for experiment)

Large $n \longrightarrow$ larger theoretical error, bad convergence of the perturbative series (it also depends on the scheme).

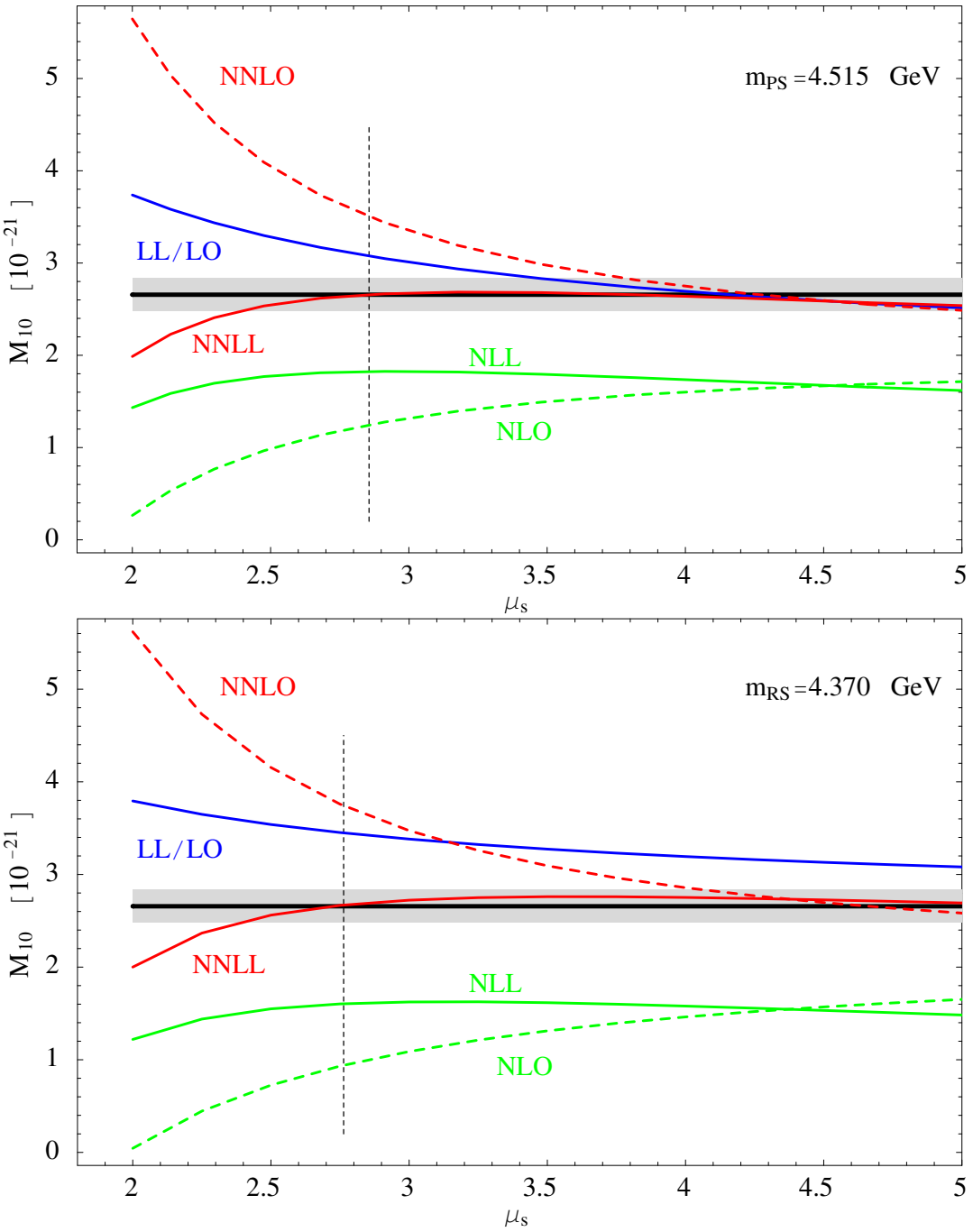

Figure 12: *The moment M_{10} as a function of μ_s at LO/LL, NLO, NLL, NNLO and NNLL for $m_{b\mathrm{PS}}(2\ \mathrm{GeV}) = 4.515\ \mathrm{GeV}$ in the PS scheme (upper figure), and for $m_{b\mathrm{RS}}(2\ \mathrm{GeV}) = 4.370\ \mathrm{GeV}$ in the RS scheme (lower figure). The experimental moment with its error is also shown (grey band).*

$$m_{b,\mathrm{PS}}(2\mathrm{GeV}) = 4.52 \pm 0.06 \ \mathrm{GeV},$$
$$m_{b,\mathrm{RS}}(2\mathrm{GeV}) = 4.37 \pm 0.07 \ \mathrm{GeV}.$$

$$\overline{m}_b(\overline{m}_b) = 4.19 \pm 0.06 \, \mathrm{GeV}.$$

The perturbative series is sign-alternating. This is the opposite than for electromagnetic decays. The convergence of the perturbative series in sum rules is also better in sum rules than for electromagnetic decays.

NNLO determinations of the bottom sum rules suffer from very huge theoretical uncertainties (which are not always incorporated in the errors): bad scale dependence and bad convergence of the perturbative series. Therefore, they can not provide precise determinations of the bottom mass.

Conclusions

Conclusions

Theoretical results

Potentials at LL and $D^{(2)}_{S^2,s}$ at NLL

Heavy quarkonium at NNLL: $m\alpha^{4+n}\ln^n\alpha$

Hyperfine splitting at NNNLL: η_b, η_c, B_c

B_s at NLL; partial NNLL

$\Gamma(V_Q(nS)\to e^+e^-)$, $\Gamma(P_Q(nS)\to\gamma\gamma)$ at NLL; partial NNLL

$\Gamma(V_Q(nS)\to e^+e^-)$ and $\Gamma(P_Q(nS)\to\gamma\gamma)$ ratio at NNLL

Applications: b-$\bar{b}$ (c-$\bar{c}$?) sum rules, t-$\bar{t}$ production, decays at NNLL (partial).

Conclusions

Theoretical results

Potentials at LL and $D^{(2)}_{S^2,s}$ at NLL

Heavy quarkonium at NNLL: $m\alpha^{4+n}\ln^n\alpha$

Hyperfine splitting at NNNLL: η_b, η_c, B_c

B_s at NLL; partial NNLL

$\Gamma(V_Q(nS)\to e^+e^-)$, $\Gamma(P_Q(nS)\to\gamma\gamma)$ at NLL; partial NNLL

$\Gamma(V_Q(nS)\to e^+e^-)$ and $\Gamma(P_Q(nS)\to\gamma\gamma)$ ratio at NNLL

Applications: b-$\bar{b}$ (c-$\bar{c}$?) sum rules, t-$\bar{t}$ production, decays at NNLL (partial).

Phenomenological analysis

RG is an important improvement

One has to be careful assigning errors: magnitude of the correction (not only soft scale dependence)

Log resummation versus finite order: t-$\bar{t}$ not really important? it looks more important for b-$\bar{b}$. One has to wait for final results at NNLL and NNNLO.

Residual strong scale dependence at relative large scales (both in t-$\bar{t}$ and bottomonium). This may hide the real importance of the resummation of logs.

Contrary to previous claims, to get an improved determination of the bottom mass RGI has to be used (or "NNNLO").

Contrary to previous claims, to get an improved determination of the top mass RGI has to be used (or "NNNLO").

Results

$$\overline{m}_b(\overline{m}_b) = 4.19 \pm 0.06\,\mathrm{GeV}.$$

Error on top mass (position of the peak): ~ 100 MeV

Error on the normalization of the total cross section: $\sim 10\%$

Results

$$\overline{m}_b(\overline{m}_b) = 4.19 \pm 0.06\,\mathrm{GeV}.$$

Error on top mass (position of the peak): ~ 100 MeV
Error on the normalization of the total cross section: $\sim 10\%$

Prospects

Potentials at NLL (some already known)
B_s at NNLL. Applications: b-$\bar{b}$ (c-$\bar{c}$?) sum rules, t-$\bar{t}$ production, inclusive production/annihilation.
$\Gamma(V_Q(nS) \to e^+e^-)$, $\Gamma(P_Q(nS) \to \gamma\gamma)$ at NNLL
Very precise determinations of m_b, m_t and α_s!! (also top-Higgs coupling).
Heavy quarkonium at NNNLL(?): $m\alpha^{5+n}\ln^n\alpha$ ($O(m\alpha^5)$ almost known: Kniehl, Penin, Smirnov, Steinhauser; Penin, Steinhauser)
Caveat of non-perturbative/ultrasoft effects (b-$\bar{b}$ physics)
Caveat on renormalon effects.

Comparison with vNRQCD results

Almost three years of disagreement and confusion.

Time: $t1 < t2 < t3$

Comparison with vNRQCD results

Almost three years of disagreement and confusion.

Time: $t1 < t2 < t3$

t1) Disagreement between pNRQCD and vNRQCD for the single (ultrasoft) leading logs in the $1/m$ and $1/m^0$ potentials.

Comparison with vNRQCD results

Almost three years of disagreement and confusion.

Time: $t1 < t2 < t3$

t1) Disagreement between pNRQCD and vNRQCD for the single (ultrasoft) leading logs in the $1/m$ and $1/m^0$ potentials.
t2) Correction of vNRQCD results.

Comparison with vNRQCD results

Almost three years of disagreement and confusion.

Time: $t1 < t2 < t3$

t1) Disagreement between pNRQCD and vNRQCD for the single (ultrasoft) leading logs in the $1/m$ and $1/m^0$ potentials.
t2) Correction of vNRQCD results.
t3) Agreement (observable: $m\alpha^5 \ln \alpha$).

Comparison with vNRQCD results

Almost three years of disagreement and confusion.

Time: $t1 < t2 < t3$

t1) Disagreement between pNRQCD and vNRQCD for the single (ultrasoft) leading logs in the $1/m$ and $1/m^0$ potentials.
t2) Correction of vNRQCD results.
t3) Agreement (observable: $m\alpha^5 \ln \alpha$).

t1a) Disagreement between pNRQCD and vNRQCD for the (ultrasoft) RG LL in the $1/m^2$ (LL), $1/m$ (NLL) and $1/m^0$ (NNLL) potentials.

Comparison with vNRQCD results

Almost three years of disagreement and confusion.

Time: $t1 < t2 < t3$

t1) Disagreement between pNRQCD and vNRQCD for the single (ultrasoft) leading logs in the $1/m$ and $1/m^0$ potentials.
t2) Correction of vNRQCD results.
t3) Agreement (observable: $m\alpha^5 \ln \alpha$).

t1a) Disagreement between pNRQCD and vNRQCD for the (ultrasoft) RG LL in the $1/m^2$ (LL), $1/m$ (NLL) and $1/m^0$ (NNLL) potentials.
t1b) Disagreement between pNRQCD and vNRQCD for the (ultrasoft) RG NLL B_s (electromagnetic current matching coefficient).

Comparison with vNRQCD results

Almost three years of disagreement and confusion.

Time: $t1 < t2 < t3$

t1) Disagreement between pNRQCD and vNRQCD for the single (ultrasoft) leading logs in the $1/m$ and $1/m^0$ potentials.
t2) Correction of vNRQCD results.
t3) Agreement (observable: $m\alpha^5 \ln \alpha$).

t1a) Disagreement between pNRQCD and vNRQCD for the (ultrasoft) RG LL in the $1/m^2$ (LL), $1/m$ (NLL) and $1/m^0$ (NNLL) potentials.
t1b) Disagreement between pNRQCD and vNRQCD for the (ultrasoft) RG NLL B_s (electromagnetic current matching coefficient).
t2) Correction of vNRQCD results.

Comparison with vNRQCD results

Almost three years of disagreement and confusion.

Time: $t1 < t2 < t3$

t1) Disagreement between pNRQCD and vNRQCD for the single (ultrasoft) leading logs in the $1/m$ and $1/m^0$ potentials.
t2) Correction of vNRQCD results.
t3) Agreement (observable: $m\alpha^5 \ln \alpha$).

t1a) Disagreement between pNRQCD and vNRQCD for the (ultrasoft) RG LL in the $1/m^2$ (LL), $1/m$ (NLL) and $1/m^0$ (NNLL) potentials.
t1b) Disagreement between pNRQCD and vNRQCD for the (ultrasoft) RG NLL B_s (electromagnetic current matching coefficient).
t2) Correction of vNRQCD results.
t3) Agreement (observable $m\alpha^{4+n} \ln^n \alpha$ (NNLL) and B_s: $\alpha^{1+n} \ln^n \alpha$ (NLL)).

Comparison with vNRQCD results

Almost three years of disagreement and confusion.

Time: $t1 < t2 < t3$

t1) Disagreement between pNRQCD and vNRQCD for the single (ultrasoft) leading logs in the $1/m$ and $1/m^0$ potentials.
t2) Correction of vNRQCD results.
t3) Agreement (observable: $m\alpha^5 \ln \alpha$).

t1a) Disagreement between pNRQCD and vNRQCD for the (ultrasoft) RG LL in the $1/m^2$ (LL), $1/m$ (NLL) and $1/m^0$ (NNLL) potentials.
t1b) Disagreement between pNRQCD and vNRQCD for the (ultrasoft) RG NLL B_s (electromagnetic current matching coefficient).
t2) Correction of vNRQCD results.
t3) Agreement (observable $m\alpha^{4+n} \ln^n \alpha$ (NNLL) and B_s: $\alpha^{1+n} \ln^n \alpha$ (NLL)).

Finally outcome: All the pNRQCD results (to date) have proven correct. The vNRQCD results have been corrected until agreement with pNRQCD results has been reached.